IEEE Access
Multidisciplinary | Rapid Review | Open Access Journal

Received 20 March 2024, accepted 21 April 2024, date of publication 15 May 2024, date of current version 4 June 2024.

Digital Object Identifier 10.1109/ACCESS.2024.3401628

RESEARCH ARTICLE

Efficient Centralized Economic Dispatch in AC/DC Interconnected Power Systems Considering Bilateral Contracts Supported by FTRs and Transmission and VSC Losses

OMAR PÉREZ ANDRADE, (Member, IEEE), JOSÉ HORACIO TOVAR HERNÁNDEZ, (Senior Member, IEEE), AND CECILE ALEJANDRA TOVAR RAMÍREZ, (Member, IEEE)

Programa de Graduados e Investigación en Ingeniería Eléctrica, Instituto Tecnológico de Morelia, Morelia, Michoacán 58120, Mexico

Corresponding author: Omar Pérez Andrade (D08120929@morelia.tecnm.mx)

This work was supported by the Consejo Nacional de Humanidades Ciencias y Tecnologías (CONAHCYT) under Grant 743277.

ABSTRACT This paper presents a formulation for performing economic dispatch (ED) in AC/DC interconnected power systems (AC/DC-IPS). Its main feature is that it uses a generalized model for power transfer distribution factors (PTDF) in such a way that its application is straightforward for AC power systems connected in either series or parallel to DC power systems. Additionally, a piecewise linear (PWL) approach is used to modeling the cost curves of the generation units and transmission losses of the entire AC/DC-IPS, comprising voltage source converters (VSC) for AC/DC links. The losses of these elements were evaluated using a linearized second-order function of the reactor current. To achieve acceptable operation of the VSCs, the control functions of programmed flow, voltage, and angular reference are enclosed in our formulation, and based on these features, a search algorithm to find ED areas is proposed, to obtain the minimum cost centralized ED for each of these areas. Moreover, bilateral contracts between producers and consumers supported by financial transmission rights (FTRs) are included in our developed model. The performance of this ED model is illustrated by two examples, concluding that our proposal is attractive for incorporation into the ED solution problem for AC/DC-IPS.

INDEX TERMS Economic dispatch, AC/DC interconnected power systems, financial transmission rights, piecewise linear, power transfer distribution factors, voltage source converters.

GLOSSARY

ACRONYMS

AARO	Affinely Adjust Robust Optimization.
AC	Alternating Current.
ADMM	Alternating Direction Method of Multipliers.
AGC	Automatic Generation Control.
BC	Bilateral Contracts.
BFA	Breadht First Algorithm.
BtB	Back-to-Back.
DC	Direct Current.
ED	Economic Dispatch.
FRS	Feasible Reconfiguration Set.
FTR	Financial Transmission Rights.
HVDC	High Voltage Direct Current.
IPS	Interconnected Power System.
ISO	Independient System Operator.
LMP	Local Marginal Cost.
LP	Linear Programming.
MILP	Mixed Integer Linear Programming.
Min	Minimizing.
MIP	Mixed Integer Programming.
MW	Mega Watt.

The associate editor coordinating the review of this manuscript and approving it for publication was Inam Nutkani.

MWh	Mega Watt hour.
OCD	Optimal Condition Descomposition.
OPF	Optimal Power Flow.
PTDF	Power Transfer Distribution Factors.
pu	per-unit.
PWL	Piecewise Linear.
SQP	Secuencial Quadratic Programming.
VSC	Voltage Source Converter.

SETS

Lg	Set of linearization segments used in the approximation of production costs.
n_{ac}	Set of nodes in the AC network.
n_{dc}	Set of nodes in the DC network.
n_{dz}	Set of dispatch zones.
ng	Set of generation units.
n_{VSC}	Set of VSCs in the IPS.

SUBSETS

n'_{ac}	Subset of AC nodes that are not terminal nodes of VSCs.
n'_{dc}	Subset of DC nodes that are not terminal nodes of VSCs.
n_{Ectrl}	Subset of VSCs with DC voltage (E) control.
n_{Pctrl}	Subset of VSCs with power flow control.
$n_{\phi ctrl}$	Subset of VSCs with angle ϕ control.

SUBSCRIPTS

$n'_{ac+1}, \ldots, n_{ac}$	Subscrip of AC nodes associated to VSC.
$n'_{dc+1}, \ldots, n_{dc}$	Subscript of DC nodes associated to VSC.

INDEXES

g	Generation unit index, 1 to $\|ng\|$.
i	AC network node index, 1 to $\|n_{ac}\|$.
j	DC network node index, 1 to $\|n_{dc}\|$.
k	Dispatch zone index, 1 to $\|n_{dz}\|$.
t	Index of AC nodes associated with VSCs, $n'_{ac+1}, \ldots, n_{ac}$.
v	Index of each VSC at the IPS.

PARAMETERS

α_v	Fixed coefficient of the loss curve of each VSC.
β_v	Linear coefficient of the loss curve of each VSC.
γ_v	Quadratic coefficient of the loss curve of each VSC.
ϕ_{ctrl}	Scheduled angle in $\text{VSC}_{\phi ctrl}$.
a_g	Fixed cost coefficient of generation for unit g.
b_g	Linear cost coefficient of generation for unit g.
B_{im}	Susceptance of the line between nodes i and m in the AC network.
B_{vsc}	Susceptance of each VSC.
BGVSC	Matrix of susceptances, conductances, and specified variables.
c_g	Quadratic cost coefficient of generation for unit g.
E_{ctrl}	Schedule voltaje in VSC_{Ectrl}.
[**F**]	Inverse of **BGVSC** matrix.
$F_{i,h}$	Element of the position of node i belonging to column h of matrix F.
G_{im}	Conductance of the line between nodes i and m in the AC network.
G_{jn}	Conductance of the line between nodes j and n of in the DC network.
G_{vsc}	Conductance of each VSC.
INS	Investigated node set.
NI	Uninvestigated node.
$NSTS$	Node-spanning tree subset.
$P^{sp}_{ac,i}$	Specified active power at node i in the AC network.
$P_{ctrl,ij}$	Power flow controlled in VSC_{Pctrl}.
$P^{sp}_{dc,j}$	Specified active power at node j in the DC network.
P_{neg}	Negotiated power.
Pac^{Max}_{im}	Maximum power flow for transmission elements from node i to m of the AC network.
Pdc^{Max}_{jn}	Maximum power flow for transmission elements from node j to n of the DC network.
$Pvsc^{Max}_{v}$	Maximum power flow for the VSC v.
$PD_{ac,i}$	Active power load at node i in the AC network.
$PD_{dc,i}$	Power load at node j in the DC network.
$PG_{ac,i}$	Active power generation at node i in the AC network.
$PG_{dc,j}$	Power generation at node j in the DC network.
PG^{Max}_{g}	Maximum active power capacity of generator g.
PG^{Min}_{g}	Minimum active power capacity of generator g.
$\mathbf{Pline}^{\mathbf{Max}}$	Vector of maximum power flow for transmission elements.
PTDF	PTDF matrix.
$PTDF_{im,h}$	Value of the PTDF corresponding to the transmission element between nodes i and m in column h of the PTDF matrix.
r_{im}	Resistance of the line between nodes i and m of in the AC network.
r_{Gmax}	Root node.
$sac_{im,l}$	Slope of segment l for the transmission element from node i to m at the AC network.
$sdc_{jn,l}$	Slope of segment l for the transmission element from node j to n at the DC network.
$sl_{g,g}$	Slope of segment lg for generation unit g in the cost modeling.

STS Spanning tree subset.
$\mathbf{SV}$ Vector of specified parameters.
$svsc_{l,v}$ Slope of segment l for the VSC v.
$voll$ Value of the lost load associated with the energy not supplied.
x_{im} Reactance of the line between nodes i and m of in the AC network.

VARIABLES

θ_i Phase angle of the complex voltage $\overline{V}_i$ at node i.
π_D LMP at node D.
π_G LMP at node G.
π_{neg} Reference LMP.
$\phi_{v,ij}$ Inner phase angle of the VSC.
$\mathbf{\Psi}$ Vector of decision variables.
$\Delta Pac_{im,l,k}$ Power flow of linear segment l at the transmission element from node i to m of the AC network within dispatch zone k.
$\Delta Pdc_{jn,l,k}$ Power flow of linear segment l at the transmission element from node j to n of the DC network within dispatch zone k.
$\Delta PG_{lg,g,k}$ Production of linear segment lg of generation unit g.
$\Delta Pvsc_{l,v,k}$ Power flow of linear segment l at the VSC v within dispatch zone k.
E_j Voltage magnitude at node j of the DC network.
I_{vsc} VSC phase current.
m'_a VSC amplitude modulation coefficient.
$P_{ac,i}$ Active power injection at node i of the AC network.
$P_{dc,j}$ Active power injection at node j of the DC network.
P_k^{loss} Total electrical losses at dispatch zone k.
$P_{vsc,i}$ VSC active power injection at node i (AC side).
$P_{vsc,j}$ VSC active power injection at node j (DC side).
P_{vsc}^{loss} VSC electrical losses.
$Pac_{im,k}$ Power flow in the transmission element from node i to m of the AC network within dispatch zone k.
$Pac_{im,k}^{+}$ Dummy positive variable representing the positive power flow in the transmission element from node i to m of the AC network within dispatch zone k.
$Pac_{im,k}^{-}$ Dummy positive variable representing the negative power flow in the transmission element from node i to m of the AC network within dispatch zone k.
$Pac_{i,k}^{loss}$ Transmission losses at node i in the AC network within zone k.
$Pac_{im,k}^{loss}$ Transmission loss in the element between nodes i and m of the AC network within zone k.
$Pdc_{jn,k}$ Power flow in the transmission element from node j to n of the DC network within dispatch zone k.
$Pdc_{jn,k}^{+}$ Dummy positive variable representing the positive power flow in the transmission element from node j to n of the DC network within dispatch zone k.
$Pdc_{jn,k}^{-}$ Dummy positive variable representing the negative power flow in the transmission element from node j to n of the DC network within dispatch zone k.
$Pdc_{j,k}^{loss}$ Transmission losses at node j in the DC network within zone k.
$Pdc_{jn,k}^{loss}$ Transmission loss in the element between nodes j and n of the DC network within zone k.
$\mathbf{Pline}$ Vector of transmission element power flows.
$\mathbf{Ploss}$ Vector of transmission network electrical losses.
R_{FTR} Payment of the FTR owner.
R_{ISO} Payment of the ISO to each FTR owner.
V_i Voltage magnitude of the complex voltage $\overline{V}_i$ at node i of the AC network.

I. INTRODUCTION

The proper integration and management of several energy resources can result in energy systems being planned and operated efficiently and covering worldwide regions, including various countries and even huge continental parts interconnected by synchronous or asynchronous links [1].

To achieve efficient operation of these very large AC/DC power systems, there is a central interest in performing economic dispatch (ED) to minimize the entire interconnected power system cost, while preserving operation limits over each of the ED areas and their tie-lines.

Similar to the ED in a single area, it is of interest to formulate an ED problem involving nonlinear production cost functions, transmission limits, and loss models. It is also necessary to incorporate AC/DC interface models, and interconnection load flow control among other features [2].

Several papers have formulated interconnected power system ED problems with a variety of different objectives. The authors of [1] emphasize in the coordination of control areas to ensure security and, at the same time, to reach a multi-area optimization with an ED and re-dispatch in congestion cases involving renewable energy sources (RES) and storage devices; simulations were performed by CPLEX and YALMIP. Reference [2] presented a distributed security-constrained unit commitment for large-scale power systems based on mixed-integer linear programming (MILP), to reduce a huge complex problem into several smaller and

simpler problems solved with parallel processing. To take advantage of complementary large-scale wind power generation, the authors of [3] presented a decentralized approach based on a modified generalized Benders decomposition for ED in an interconnected power system (IPS) incorporating various dispatch areas. In addition, a coordination framework for dispatch and tie-line scheduling to operate multi-area power systems in the presence of large-scale wind farms was proposed in [4] and solved using a two-stage adaptive robust optimization. Reference [5] focused on calculating the operational risk due to uncertainty in settling wind power by coordinating multi-area generation and reserves resources using loss of load and wind spillage probability indexes and considering the optimality condition decomposition (OCD) technique to obtain an efficient solution algorithm based on MILP. In [6], a decentralized optimal transmission switching was proposed to mitigate and manage congestion during the real-time operation of multi-area power systems, and considering contingencies over the interconnected power systems, which is solved by using mixed integer programming (MIP) and Bender's decomposition, while observing as limited the private information of each independent system operator (ISO). Furthermore, the authors of [7] developed a distributed economic model for a predictive control strategy for ED and load frequency control of interconnected power systems (IPS), which achieves real-time and transient optimization involving generation, frequency control, and tie-line costs.

However, some studies have focused on the development of optimization models involving either the preservation of control area responsibilities [1] or the autonomy of each area in an IPS [4], [8]. In this sense, [9] encompassed the more specific interaction rules between North American markets, while [10] formulated a multi-objective multi-area ED problem solved by a hybrid evolutionary algorithm based on the shuffle frog-leaping algorithm involving a particle swarm optimization method. Reference [11] proposed an approach to reflect the scheduling decisions of multiple system operators (ISOs), where each ISO manages limited information regarding the other ones. Additionally, [12] proposed a day-ahead optimization model for the IPS, considering the spatial clustering effect of renewable energy resources and loads, and used robust optimization theory by formulating a hybrid evolutionary filter optimization to solve the mixed-integer non-convex nonlinear programming problem.

Reference [13] presented a decentralized robust dispatch method for a multi-area AC/DC power system considering wind power uncertainty and an affinely adjustable robust optimization (AARO) model, which simultaneously includes optimized participation factors for automatic generation control (AGC) to ensure the operational reliability of the entire system, whose regional dispatch areas interconnect with others by controlled HVDC links. The resulting proposal is a fully decentralized parallel scheme based on the accelerated alternating direction method of multipliers (ADMM). The authors of [14] developed an optimization model to allocate 100% renewable generation worldwide, through a simplified AC/DC transmission network.

Moreover, [15] presents a great overview of multi-area ED, emphasizing the main characteristics of centralized and decentralized ED, including political, technical, huge amounts of information, privacy of some data, and independence decisions. This reference lists several evolutive, dynamic, and hybrid algorithms for solving the ED problem, which consider different objective functions, and their formulation is either centralized or decentralized.

From the above references, it is important to point out that almost all of them use some variants of either MILP or evolutionary optimization to solve the ED problem in the IPS, and there are various proposals for making more suitable and efficient solution algorithms using decomposition methods. Furthermore, only [12] and [13] considered transmission AC/DC networks in their optimization models for ED in AC/DC-IPS, but they did not consider the different control modes of HVDC-VSC links and, as shown later in this paper, there are some references that assume the VSC control modes for solving the ED, but only for single AC/DC power systems, that is, not for IPS.

It is important to note that references [1], [2], [3], [7], [8], [10], [11], and [14] formulate a kind of ED problem in AC power systems, but they do not include power transmission distribution factors (PTDFs). Reference [15] reviewed many proposals for solving ED and it does not mention something about the PTDFs utilization. Moreover, the authors of [4], [6], and [9] formulate the ED problem for AC power systems incorporating PTDFs, while ED for AC/DC power systems without the inclusion of PTDFs was presented in [12], [13], [16], [17], and [18]. By the other hand, proposals to use PTDFs in AC/DC power systems for solving contingency analysis [19], ED [20], and unit commitment [21]. In these four cases, the PTDFs of the AC and DC networks are calculated in a separate fashion and their models are connected by a proper modification of the independent vector in the linear network model, depending on the control mode adopted for the VSCs.

It is apparent that almost of the ED proposals are based on some linear programming (LP) variant, because of their advantages over the nonlinear ED formulations [22]. This fact has conducted to split quadratic cost functions of generators in several linear segments by using a piecewise linear (PWL) technique [19], [20], [21], [23], being the most applied the evenly spaced piecewise linear (ES-PWL) interpolation method, as analyzed in [22]. In the same direction for solving the ED problem with LP algorithms, a proposal for representing transmission losses as PWL segments from a quadratic function involving the power flow is developed in [24]. Reference [25] linearizes the quadratic loss function at each transmission line in terms of the angular difference between its nodes, the slope and value of each linear

segment (block). Additionally, the authors of [26] carried out an investigation of two PWL methods, the ES-PWL and a combination of this technique with the tangent ES-PWL in order to reduce the over-estimation error of the former, based on the quadratic loss function of [24], and references [20], [21], and [23] utilize this same function for AC/DC power systems.

Considering an electricity market framework, in some countries as the United States it is common to find electrical energy transactions between participants pertaining to different electricity markets [27], where these transactions are formalized through the sign of bilateral contracts, and the use of financial transmission rights [28]; moreover, there is a bilateral contract between the Federal Commission of Electricity (CFE, Mexico) and the National Institute of Electricity (INDE, Guatemala) [29], just for mentioning some of this kind of contracts, which are fixed in the quantity of point-to-point power transferred, consider a reference price, and the nodal prices at their AC interconnection sending/receipt nodes calculated by the optimization model of the day ahead of each market involved. For all these cases mentioned above, all the interconnections are AC transmission lines, and the transactions are firm, i.e., with a physical capacity of these lines dedicated exclusively to support these transactions [28]. However, it is known that only HVDC links are capable of control power flow effectively, especially the VSC-HVDC technology [30], so that it would be interesting to incorporate this transmission devices for the power flow control in the electricity market context.

From the above review, and despite the handicaps of a centralized ED, in this paper, the formulation of an AC/DC-IPS centralized ED problem is proposed. The optimization model considers that all the necessary data are available. The model comprises quadratic production cost and transmission loss functions linearized by a PWL technique suitable to apply an LP algorithm to solve it [24], [26]. The optimization model includes an algorithm that considers the VSC control modes, which permit the definition of one or more dispatch areas to make it easier to solve the problem efficiently. Furthermore, our proposal uses a general power transfer distribution factors (PTDF) method to reduce the number of decision variables to make the solution more efficient.

Contributions: According to the state of the art presented above, from the knowledge of the authors of the present work, our contributions are as follows:

1. An approach based on a search algorithm for defining the dispatch zone number for AC/DC-IPS is different from the proposals of the consulted references, whose procedures use decomposition techniques or explicitly assume that the AC/DC-IPS has one or more dispatch zones.
2. A virtual generator is added to each ED zone to guarantee that there will always be a power balance in the AC/DC-IPS, where each virtual generator is allocated at the AC node of the VSC operating as a power-flow controller and delimiting its corresponding dispatch zone.

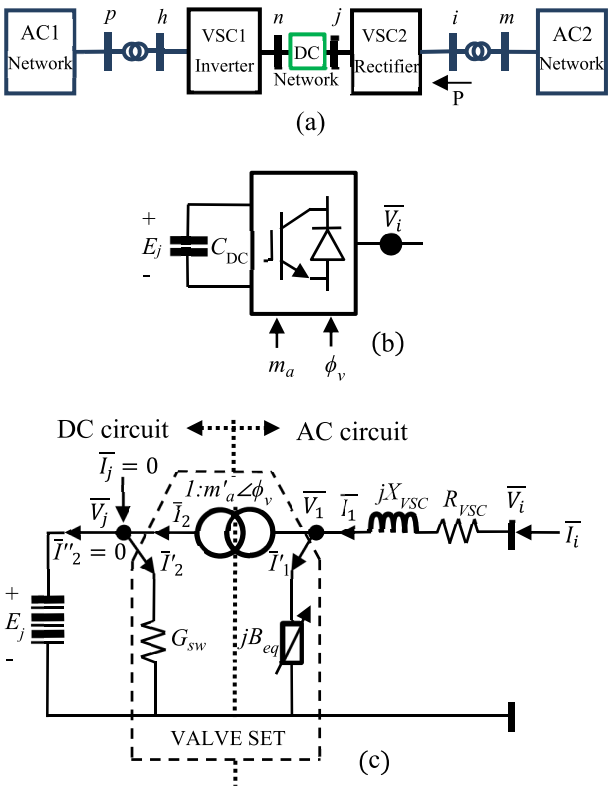

FIGURE 1. AC/DC interconnected system: (a) Two AC networks interconnected through two VSCs and a DC network, (b) VSC schematic representation by electric circuits [31], and (c) VSC steady-state equivalent circuit.

3. A generalized PTDF calculation model was developed for the AC/DC network of each ED area, including the control modes of the VSC devices. This process is computationally more efficient than the PTDF determination for the whole AC/DC-IPS.
4. In the application of LP to solve the ED problem, it is common for generation cost curves and transmission losses, including VSCs, to be represented by different PWL techniques. In this study, both curve types were linearized exactly with the same PWL technique, and the results show that there is no need to develop a specific PWL technique for each type of curve.
5. The application of bilateral contracts involving FTRs for AC/DC-IPS is illustrated, showing the usefulness of these concepts even when dispatch is realized only for each ED area.

II. INJECTED NODAL ACTIVE POWER EQUATIONS DEL AC/DC-IPS

Fig. 1(a) depicts an AC/DC-IPS interconnecting two AC networks interchanging the active power P from AC2 to AC1 through a HVDC link constituted by a VSC rectifier (VSC2), a DC network, and a VSC inverter (VSC1). Figs. 1(b) and 1(c) show the VSC representation by circuit elements [31]. In the case of a back-to-back VSC array, the DC network is a common node (nodes *n* and *j* are the same).

In the steady-state operation of the AC/DC-IPS, involving any number of converters VSC stations, the calculation of active power injection at each node of the AC and DC networks and VSC stations is as follows:

$$P_{ac,i} = V_i \sum_{m \in i} V_m \left[G_{im} cos\left(\theta_{im}\right) + B_{im} sin\left(\theta_{im}\right)\right]; \quad i = 1, \ldots, n_{ac} \tag{1}$$

where $\theta_{im} = (\theta_i - \theta_m)$ and θ_i, θ_m are the phase angles of the complex voltages $\overline{V_i}$, $\overline{V_m}$, $G_{im} + \mathrm{j}B_{im} = (r_{im} + \mathrm{j}x_{im})^{-1}$, $G_{ii} = -\sum_{m \in i} G_{im}$, $B_{ii} = -\sum_{m \in i} B_{im}$, and n_{ca} is the number of AC nodes. Similarly, for all DC nodes.

$$P_{dc,j} = E_j \sum_{n \in j} E_n G_{jn}; \quad j = 1, \ldots, n_{dc} \tag{2}$$

where $G_{jn} = -\left(r_{jn}\right)^{-1}$, $G_{jj} = \sum_{n \in j} G_{jn}$. Furthermore, considering the circuit show in Fig. 1(c), the equations of active power injections at nodes i (AC side) and j (DC side) of each VSC involved in the AC/DC-IPS are:

$$P_{vsc,i} = V_i^2 G_{vsc} - m'_a V_j V_i \left[G_{vsc} \cos\left(\theta_i - \phi_{v,ij}\right) + B_{vsc} \sin\left(\theta_i - \phi_{v,ij}\right)\right] \tag{3}$$

$$P_{vsc,j} = -m'_a V_i V_j \left[G_{vsc} \cos\left(\phi_{v,ij} + \theta_j\right) + V_j^2 \left(G_{sw} + m_a^{'2} G_{vsc}\right) + B_{vsc} \sin\left(\phi_{v,ij} + \theta_j\right)\right] \tag{4}$$

where $\phi_{v,ij}$ is the inner phase angle of the converter, $\theta_{ji} = -\theta_{ij}$, and $G_{vsc} + \mathrm{j}B_{vsc} = (r_{vsc} + \mathrm{j}x_{vsc})^{-1}$. Additionally, to obtain the complete active power injected at nodes i and j, it is necessary to sum equations (1) and (3) and to sum (2) and (4), respectively.

For additional VSC devices, there should be another proper node pair instead of nodes i, j in Equations (1)–(4).

A. LINEAR INJECTED ACTIVE POWER EQUATIONS OF THE AC/DC-IPS

There is a well-known set of assumptions for obtaining a linear set of equations (1) − (4), which are as follows [16], [17]:

1) In AC networks, line series-resistance, shunt capacitors and reactors are omitted, and all the transformer load tap changers are at their nominal value, i.e., at 1.0 pu in the per unit system.
2) The voltage magnitude in all the AC nodes is assumed as 1.0 pu, and in a similar fashion, $V_j m'_a = E_{jCD} m'_a \approx 1$pu in the VSC DC nodes.
3) The angular difference between adjacent AC voltage phasor nodes is relatively small; therefore, $sin\left(\theta_i - \phi_{v,ij}\right) \approx \left(\theta_i - \phi_{v,ij}\right)$ and $sin\left(\theta_{im}\right) \approx \left(\theta_{im}\right)$.
4) For DC networks, a lossless transmission line model can be obtained by considering that the current across the line is approximately equal to the active power flow in terms of the per-unit system, that is, $I_{dc,j} \approx P_{dc,j}$ in pu [17].

Applying the above suppositions, (1)–(4) result in linear equations (5)–(8), respectively [16].

$$P_{ac,i} = \sum_{\substack{m \in i \\ m \neq j}} B_{im}\left(\theta_{im}\right); \quad i = 1, \ldots, n_{ac} \tag{5}$$

$$P_{dc,j} = \sum_{\substack{n \in j \\ n \neq i}} G_{jn}\left(E_j - E_n\right); \quad j = 1, \ldots, n_{dc} \tag{6}$$

$$P_{vsc,i} = B_{vsc}\left(\theta_i - \phi_{v,ij}\right) \tag{7}$$

$$P_{vsc,j} = B_{vsc}\left(\phi_{v,ij} - \theta_i\right) = -B_{vsc}\left(\theta_i - \phi_{v,ij}\right) \tag{8}$$

where $B_{im} = -x_{im}^{-1}$; $B_{ii} = \sum_{m \in i} x_{im}^{-1} i = 1, \ldots, n_{ca}$; $B_{vsc} = x_{vsc}^{-1}$.

If there is no VSC converter connected to nodes i and j, then Equations (9)–(10) are the active power nodal balance in each node of the AC and DC networks, respectively.

$$PG_{ac,i} - PD_{ac,i} - P_{ac,i} = P_{ac,i}^{sp} - P_{ac,i} = 0; \quad i = 1, \ldots, n'_{ac} \tag{9}$$

$$PG_{dc,i} - PD_{dc,i} - P_{dc,i} = P_{dc,j}^{sp} - P_{dc,j} = 0; \quad j = 1, \ldots, n'_{dc} \tag{10}$$

where n'_{ac} and n'_{dc} are the AC and DC nodes in the IPS without the nodes associated to VSC interconnected to them; $P_{ac,i}^{sp}$ and $P_{dc,j}^{sp}$ are the specified active powers, while $PG_{ac,i}$, $PG_{dc,j}$, $PD_{ac,i}$, $PD_{dc,j}$, are the generation and load active powers in AC and DC nodes, respectively.

Moreover, for each VSC interconnecting nodes i and j, the last two equations should include the VSC active power injections, resulting in Eqs. (11) and (12).

$$P_{ac,i}^{sp} - P_{ac,i} - P_{vsc,i} = 0; \quad i = n'_{ac+1}, \ldots, n_{ac} \tag{11}$$

$$P_{dc,j}^{sp} - P_{dc,j} - P_{vsc,j} = 0; \quad j = n'_{dc+1}, \ldots, n_{dc} \tag{12}$$

where $P_{vsc,i} = B_{vsc}\left(\theta_i - \phi_v\right)$ and $P_{vsc,j} = B_{vsc}\left(\phi_v - \theta_i\right)$, and subscripts for AC and DC nodes associated to VSC converters run from $n'_{ac+1}, \ldots, n_{ac}$ and $n'_{dc+1}, \ldots, n_{dc}$, respectively.

B. CONVERTER CONTROL MODES

VSCs can be controlled to maximize benefits for the interconnected power system. Therefore, it is crucial to establish the operational conditions under which the interconnected power system operates. Firstly, it should be acknowledged that these systems aim to efficiently utilize generation resources in each respective region. Consequently, it is natural to have participants in a global market, where some generate electricity and others consume it, establishing buy-sell relationships (transactions) among them, belonging to different power systems.

In general terms, in wholesale electricity markets, energy transactions between agents from different markets and, consequently, power systems, can be classified into two types: firm and non-firm transactions. Non-firm transactions do not guarantee the supply of the contracted energy to the buying party due to technical or dispatch considerations. On the other hand, firm transactions must be carried out regardless of the operational conditions and load levels of interconnected

power systems. To achieve this goal, the independent system operator reserves transfer capacity by establishing a pathway between the interconnections of the involved systems. This is achieved by specifying the power flow through the interconnection as a constraint, which can be controlled by an interconnection VSC. In this way, the necessary transfer capacity is reserved to make each firm transaction possible.

In this context, this reserved transfer capacity can be seen as the sum of the scheduled firm transactions through the same VSC, that is, $P_{ctrl_i} = \sum T_{tjk}$, where j is the sending node and k is the receiving node.

Multiterminal VSC systems permit the application of different strategies or control modes to accomplish the operative requirements between the AC and DC transmission networks.

The control mode representation is obtained by the aggregation of the equality constraint, which depends on the selected control mode [16], as shown below.

(i) Power flow control. A VSC under this control mode is defined as a VSC$_{Pctrl}$ and involves the following equation:

$$P_{ctrl,ij} = B_{VSC}\left(\theta_i - \phi_{v,ij}\right) \tag{13}$$

where $P_{ctrl,ij}$, expressed in pu or MW, is the power flow through nodes i to j, which is controlled by adjusting of the angular difference in (13).
One of the objectives of this article is the inclusion of aspects related to the energy trading among agents participating in electricity markets associated with different power systems. One of the most common methods for conducting these transactions as firm through well-defined pathways between the interconnections of such power systems with power flow controlled VSCs.

(ii) Angular reference control. A VSC converter can provide an angular reference to the AC node i, denoted as VSCϕ_{ctrl}, and its corresponding equality constraint is

$$\phi_{ctrl} = \phi_{v,ij} \tag{14}$$

where the scheduled angle ϕ_{ctrl} is rad. This control mode is reflected directly by incorporating B_{VSC} with the signs of Equations (7) and (8), according to the position of $\phi_{v,ij}$ into the variable vector of the linearized Equation (16).

(iii) DC voltage control. Any converter denoted as VSC$_{Ectrl}$, has the capability of controlling the node j in the DC network, so that, the equality constraint is:

$$E_{ctrl} = E_j \tag{15}$$

where the units of scheduled voltage E_{ctrl} are in pu. This restriction is integrated into the coefficient matrix of (16) by assigning a value of 1.0 in the corresponding diagonal position with respect to the position of E_j in the variable vector.

These control modes are illustrated in the study cases.

For instance, we can have predefined firm energy transactions through VSC links operating in power flow control mode. In addition to these transactions, there may be unplanned or predefined energy exchanges or trading, with VSCs operating in either voltage control or angle control modes. There could be dispatch zones that import or export energy. If the power flows associated with these zones are predefined, then power flow control mode is utilized; otherwise, the other two control modes are employed.

Angle control mode is used to establish a reference in the corresponding dispatch zone for all AC nodes, regardless of whether the zone imports or exports energy. Under this condition, the resulting dispatch angles have values that are consistent with angles obtained with a conventional power flow algorithm. Otherwise, it has been observed that the values of these angles can be highly deviated from common values, leading to potentially erroneous conclusions about the steady-state stability of the interconnected power system [19].

Additionally, it is important to note that there could be any number of VSC converters, but each one will adopt one of the control modes. Therefore, the number of VSC converters will be $n_{VSC} = n_{Pctrl} + n_{\phi ctrl} + n_{Ectrl}$.

C. MATRIX NOTATION

In the compact matrix and vector terms, Equation (16) represents linear equations (9)–(15).

$$[\mathbf{SV}] = [\mathbf{BGVSC}]\,[\mathbf{\Psi}] \tag{16}$$

where vectors [**SV**] and [$\mathbf{\Psi}$] are as follows:

$$[\mathbf{SV}] = \left\{ \begin{array}{c} \begin{bmatrix} PG_{ac,1} - PD_{ac,1} \\ \vdots \\ PG_{ac,n'_{ac}} - PD_{ac,n'_{ac}} \end{bmatrix} \\ \begin{bmatrix} PG_{ac,n'_{ac}+1} - PD_{ac,n'_{ac}+1} \\ \vdots \\ PG_{ac,n_{ac}} - PD_{ac,n_{ac}} \end{bmatrix} \\ [P_{ctrl}] \\ [\phi_{ctrl}] \\ [E_{ctrl}] \\ \begin{bmatrix} PG_{dc,1} - PD_{dc,1} \\ \vdots \\ PG_{dc,n'_{dc}} - PD_{dc,n'_{dc}} \end{bmatrix} \\ \begin{bmatrix} PG_{dc,n'_{dc}+1} - PD_{dc,n'_{dc}+1} \\ \vdots \\ PG_{dc,n_{dc}} - PD_{dc,n_{dc}} \end{bmatrix} \end{array} \right\};$$

$$[\boldsymbol{\Psi}] = \left\{ \begin{bmatrix} \theta_1 \\ \vdots \\ \theta_{n'_{dc}} \end{bmatrix} \begin{bmatrix} \theta_{n'_{dc}+1} \\ \vdots \\ \theta_{n_{dc}} \end{bmatrix} \begin{bmatrix} \phi_1 \\ \vdots \\ \phi_{n_{vsc}} \end{bmatrix} \begin{bmatrix} E_{1_{dc}} \\ \vdots \\ E_{n'_{dc}} \end{bmatrix} \begin{bmatrix} E_{n'_{dc}+1} \\ \vdots \\ E_{n_{dc}} \end{bmatrix} \right\} \tag{17}$$

Additionally, matrix [**BGVSC**] has the structure shown in equation (18), at the bottom of the next page.

where the sub-matrices [**' 0**] are null while maintaining a proper order. Moreover, the remaining submatrix definitions are

$$[\mathbf{B}_{Iac}] = \begin{bmatrix} B_{1,1} & \cdots & B_{1,n'_{ac}} \\ \vdots & \ddots & \vdots \\ B_{n'_{ac},1} & \cdots & B_{n'_{ac},n'_{ac}} \end{bmatrix} \tag{19}$$

$$[\mathbf{B}_{IIac}] = \begin{bmatrix} B_{i,n'_{ac}+1} & \cdots & B_{i,n_{ac}} \\ \vdots & \ddots & \vdots \\ B_{n'_{ac},n'_{ac}+1} & \cdots & B_{n'_{ac},n_{ac}} \end{bmatrix} \tag{20}$$

$$[\mathbf{B}_{IIIac}] = \begin{bmatrix} B_{n'_{ac}+1,i} & \cdots & B_{n'_{ac}+1,n'_{ac}} \\ \vdots & \ddots & \vdots \\ B_{n_{ac},i} & \cdots & B_{n_{ac},n'_{ac}} \end{bmatrix} \tag{21}$$

$$[\mathbf{B}_{IVac}] = \begin{bmatrix} B_{n'_{ac}+1,n'_{ac}+1}+B_{vsc,v} & \cdots & 0 \\ \vdots & \ddots & \vdots \\ 0 & \cdots & B_{n_{ac},n_{ac}}+B_{vsc,n_{vsc}} \end{bmatrix} \tag{22}$$

$$[\mathbf{B}_{v}] = \begin{bmatrix} B_{vsc,v} & \cdots & 0 \\ \vdots & \ddots & \vdots \\ 0 & \cdots & B_{vsc,n_{vsc}} \end{bmatrix} \tag{23}$$

$$[\mathbf{G}_{Idc}] = \begin{bmatrix} G_{1_{dc},1_{cd}} & \cdots & G_{1_{dc},n'_{dc}} \\ \vdots & \ddots & \vdots \\ G_{n'_{dc},1_{dc}} & \cdots & G_{n'_{dc},n'_{dc}} \end{bmatrix} \tag{24}$$

$$[\mathbf{G}_{IIdc}] = \begin{bmatrix} G_{j,n'_{dc}+1} & \cdots & G_{j_{dc},n_{dc}} \\ \vdots & \ddots & \vdots \\ G_{n'_{dc},n'_{dc}+1} & \cdots & G_{n'_{dc},n_{dc}} \end{bmatrix} \tag{25}$$

$$[\mathbf{G}_{IIIdc}] = \begin{bmatrix} G_{n'_{dc}+1,j} & \cdots & G_{n'_{dc}+1,n'_{dc}} \\ \vdots & \ddots & \vdots \\ G_{n_{dc},j} & \cdots & G_{n_{dc},n'_{dc}} \end{bmatrix} \tag{26}$$

$$[\mathbf{G}_{IVdc}] = \begin{bmatrix} G_{n'_{dc}+1,n'_{dc}+1} & \cdots & G_{n'_{dc}+1,n_{dc}} \\ \vdots & \ddots & \vdots \\ G_{n_{dc},n'_{dc}+1} & \cdots & G_{n_{dc},n_{dc}} \end{bmatrix} \tag{27}$$

$$[\mathbf{VSC}_{P}] = \begin{bmatrix} B_{vsc} & \cdots & 0 & \cdots & 0 \end{bmatrix} \tag{28}$$

$$[\mathbf{VSC}_{\phi}] = \begin{bmatrix} 0 & \cdots & 1 & \cdots & 0 \end{bmatrix} \tag{29}$$

$$[\mathbf{VSC}_{E}] = \begin{bmatrix} 0 & \cdots & 0 & \cdots & 1 \end{bmatrix} \tag{30}$$

Note that for each AC node assigned as a slack node, we should omit the corresponding row and column in the matrix [**BGVSC**].

Solution of equations (16) is straightforward, i.e., $[\boldsymbol{\Psi}] = [\mathbf{BGVSC}]^{-1}[\mathbf{SV}] = [\mathbf{F}][\mathbf{SV}]$, and then $[\mathbf{F}] = [\mathbf{BGVSC}]^{-1}$.

D. DETERMINATION OF POWER TRANSFER DISTRIBUTION FACTORS (PTDF)

PTDF calculus considers the matrix [**F**], where each PTDF determination depends on the values of the corresponding entries, as explained below [20], [32].

For AC transmission elements connecting any pair of nodes, i, m:

$$PTDF_{im,h} = B_{im}\left(F_{i,h} - F_{m,h}\right) \tag{31}$$

Equation (31) indicates that there is a power flow across element i, m caused by a power injection at node k. Additionally, there is a similar calculation of PTDFs in any transmission line connecting nodes j, n in the DC network(s):

$$PTDF_{jn,h} = G_{jn}\left(F_{j,h} - F_{n,h}\right) \tag{32}$$

First, the dimensions of the PTDF matrix, denoted as [**PTDF**], are equal to the total number of AC/DC-IPS transmission elements $L_{ac/dc}$, by the total number of its nodes, that is, $\left(L_{ac/dc}\right) \times (n_{ac} + n_{dc} + n_{vsc})$. However, as explained later, these dimensions are smaller if there is more than one dispatch zone.

III. ECONOMIC DISPATCH PROPOSAL

The basic goal of ED is to calculate the most economically active power production of generation plants to satisfy the system load and supply all the electrical losses, while keeping all the imposed technical constraints on the problem formulation [16], [17], [20]. As a first step, this section includes an algorithm for searching each dispatch zone in the AC/DC-IPS. Moreover, a detailed model for considering electrical losses in VSC converters and transmission elements in AC and DC networks is presented. Finally, the proposed model for ED is formulated to solve the resulting mathematical model using an LP solver.

A. DETERMINATION OF DISPATCH ZONES

A dispatch zone is characterized by possessing a set of self-owned generators with the capacity to meet demand, and it may even have surplus generation ready for export. In case of a generation deficit within the zone, it can import energy to fulfill its entire demand through interconnections with other power systems.

The procedure for the determination of dispatch zones consists of finding, by using a topological search algorithm, all the dispatch zones that exist in the AC/DC-IPS, where each one will have an AC reference node and a term in the objective function associated with the unsupplied energy. The cardinality concept of theory sets forms the basis for the development of a search algorithm.

In terms of graph theory, an AC/DC-IPS, that is, a meshed network, is represented by a graph formed by branches and links that connect vertices (nodes). Thus, if the links are separated from the graph, the result is a graph with only one trajectory between any two nodes in the graph. If this graph includes all AC/DC power system nodes, then the graph is a connected tree graph or spanning tree [33].

Defining the branch number as B, link number as L, and their extreme points (nodes), whose number is M, therefore, the spanning-tree graph has $M-1=B$ branches. If the search algorithm finds only a spanning-tree, there will be only one ED zone. If the result is a disconnected graph, there will be more than one ED zone.

With graph information and using a breadth-first search algorithm (BFA), the search process developed for finding the feasible reconfiguration set *(FRS)* is described as follows.

1. Initial conditions. Set $n_{dz}=1$. The generation nodes select the node that has the largest maximum capacity, called as $r_{Gmax}^{n_{dz}}$, and define it as the root node of the node-spanning tree subset $NSTS^{n_{dz}}=\{r_{Gmax}^{n_{dz}}\}$. This node is labeled as an uninvestigated node (NI node). Moreover, the spanning tree subset $\left|STS^{n_{dz}-1}\right|=0$, $STS^{n_{dz}}=\{\emptyset\}$, which is empty at this stage. Create an investigated node set, $INS=\{\emptyset\}$. Set $STS^{n_{dz}}$ cardinality, $\left|STS^{(0)}\right|=0$.
2. AC/DC power system graph construction. Create the corresponding graph of the AC/DC power system, considering that each VSC operating as $\text{VSC}_{\phi ctrl}$ or VSC_{Ectrl}, is interconnecting its two extreme nodes with a closed branch. If the VSC operates as a VSC_{Pctrl}, then the branch between its two extreme nodes is open.
3. Select the first NI node from $NSTS^{n_{dz}}$, defined as n_i, i.e., $n_i \notin INS$, and find all its incident closed branches, $(n_i,n_1),(n_i,n_2),\ldots$, in order to create a neighbor node subset, $NNS=\{n_1,n_2,\ldots\}$. Take n_1 and try to find it in $NSTS^{n_{dz}}$. If $n_1 \notin NSTS^{n_{dz}}$, add it to this set and update $STS^{n_{dz}}=STS^{n_{dz}}\cup\{(n_i,n_1)\}$, and $INS=INS\cup\{n_1\}$; otherwise, select n_2 and repeat this procedure, and so on, until all nodes in NNS are investigated.
4. If in step 3, a new node n_k, go to step 3.
5. Modify $\left|STS^{n_{dz}+1}\right|=\left|STS^{n_{dz}-1}\right|+\left|STS^{n_{dz}}\right|$. If $\left|STS^{n_{dz}+1}\right|=M-1$, then the BFA finishes, and all dispatch zones are found for the AC/DC power system. Go to step 6. Otherwise, find one node not included in $NSTS^{n_{dz}}$, update $n_{dz}=n_{dz}+1$. Let this node be r_{new}, so therefore, $NSTS^{n_{dz}}=\{r_{new}\}$, and repeat Step 3.
6. The last step is the automatic assignation of one slack node to the $k=2,\ldots,n_{dz}$ dispatch zones, which are selected as the largest capacity generators at each one of them. In the case that in a particular ED zone there is no any generator or total load is greater than the sum of all generator maximum capacities, there should be a VSC operating in the $\text{VSC}_{\phi ctrl}$ mode. This action permits the compensation of total load and losses in that ED zone and, for the sake of security, this VSC is connected to a virtual generator with sufficient capacity to make the ED solution feasible in that ED zone. For each ED zone, at the AC node terminal of one of its corresponding VSC, there is a connected virtual generator.

Finally, it is important to note that the centralized ED solution arrives in terms of the dispatch zones determined by the search algorithm, so that the computational burden is less than the complete original problem because all the matrices and vectors (17)–(30) have dimensions smaller than the only dispatch zone problem, which also applies to the PTDFs calculations. Results of this centralized ED problem is automatically sent to the system operator, for its reviewing and final approval.

If the operator is aware of the control mode of their converters, he could determine dispatchable areas based on that system knowledge. In this scenario, the added value of our algorithm in identifying dispatch zones would be in its ability to perform this task in an automated and efficient manner. This is achieved by independently solving the ED for each one of the dispatchable areas, providing a faster and more accurate tool for identifying and managing dispatchable areas in the system.

B. VSC ELECTRICAL LOSS MODELING

During the AC/DC or DC/AC conversion process, the active power extracted on one side of the VSC will be less than the injected active power into the other side, owing to converter electrical losses P_{vsc}^{loss}. The authors of [18] and [34] defined these losses as a quadratic function depending on

$$[\mathbf{BGVSC}]=\begin{Bmatrix} [\mathbf{B}_{Iac}] & [\mathbf{B}_{IIac}] & [\mathbf{0}] & [\mathbf{0}] & [\mathbf{0}] \\ [\mathbf{B}_{IIIac}] & [\mathbf{B}_{IVac}] & -[\mathbf{B}_v] & [\mathbf{0}] & [\mathbf{0}] \\ [\mathbf{0}] & -[\mathbf{VSC}_P] & [\mathbf{VSC}_P] & [\mathbf{0}] & [\mathbf{0}] \\ [\mathbf{0}] & [\mathbf{0}] & [\mathbf{VSC}_\phi] & [\mathbf{0}] & [\mathbf{0}] \\ [\mathbf{0}] & [\mathbf{0}] & [\mathbf{0}] & [\mathbf{0}] & [\mathbf{VSC}_E] \\ [\mathbf{0}] & [\mathbf{0}] & [\mathbf{0}] & [\mathbf{G}_{Idc}] & [\mathbf{G}_{IIdc}] \\ [\mathbf{0}] & -[\mathbf{B}_v] & [\mathbf{B}_v] & [\mathbf{G}_{IIIdc}] & [\mathbf{G}_{IVdc}] \end{Bmatrix} \tag{18}$$

the value and direction of the converter phase current, I_{vsc}. These current changes if the VSC acts either as a rectifier or inverter, which results in different polynomial coefficients. In general, the mathematical expression for modeling VSC electrical losses is

$$P_{vsc}^{loss} = \alpha_v + \beta_v |I_{vsc}| + \gamma_v I_{vsc}^2 \tag{33}$$

where α_v, β_v and γ_v are polynomial coefficients, and γ_v will have a different value if the VSC operates either as a rectifier or inverter. Furthermore, assuming that $I_{vsc,i} \approx P_{vsc,i}$ in the per-unit system, we can write Equation (33) in terms of power:

$$P_{vsc}^{loss} = \alpha_v + \beta_v |P_{vsc,i}| + \gamma_v P_{vsc,i}^2 \tag{34}$$

C. OBJETIVE FUNCTION

The objective function of the ED problem is to minimize the active power production costs, as described in Equation (35) [20].

$$Min \sum_{k=1}^{n_{dz}} \left[\sum_{g=1}^{ng} \left(a_g + \sum_{lg \in Lg} s_{lg,g} \Delta PG_{lg,g,k} \right) + \sum_{t=n'_{ac+1}}^{n_{ac}} voll_{t,k} \left(ENS_{t,k} \right) \right] \tag{35}$$

where:

$$s_{lg,g} = (2lg - 1)\, c_g \left(PG_g^{Max} \Big/ Lg \right) + b_g; lg = 1, \ldots, Lg; g = 1, \ldots, ng \tag{36}$$

In the two above equations, a_g, b_g and c_g are coefficients of the quadratic cost function, PG_g^{Max} is the maximum active power capacity of generator g, $\Delta PG_{lg,g,k}$ is the lg linear section of the active power of generator g located at dispatch zone k, and $s_{lg,g}$ is its slope. Moreover, *voll* is the value of the lost load associated with the energy not supplied, ENS_k, which is produced by the virtual generator located in dispatch zone k.

D. ACTIVE POWER BALANCE

In optimal power flow (OPF) formulations based on PTDF, computation of the optimal solution utilizes a global equality constraint, as shown in equations (37) and (38), considering all the generation and load nodal injections and transmission losses in the AC/DC-IPS.

$$\sum_{g=1}^{ng} PG_{g,k} + \sum_{t=n'_{ac+1}}^{n_{ac}} ENS_{t,k} = \sum_{i=1}^{n_{ac}} PD_{i,k} + \sum_{j=1}^{n_{dc}} PD_{j,k} + P_k^{loss}; \quad k = 1, \ldots, n_{dz} \tag{37}$$

$$P_k^{loss} = \sum_{i=1}^{n_{ac}} Pac_{i,k}^{loss} + \sum_{j=1}^{n_{dc}} Pdc_{j,k}^{loss} + \sum_{v=1}^{n_{vsc}} Pvsc_{v,k}^{loss}; \quad \forall k = 1, \ldots, n_{dz} \tag{38}$$

where P_k^{loss} in (37) is the total electrical loss at dispatch zone k, broken down in (38) as transmission losses in the AC and DC network(s), $Pac_{i,k}^{loss}$, $Pdc_{j,k}^{loss}$, respectively, and VSC converters, $Pvsc_{v,k}^{loss}$.

In this case, for every transmission element of AC and DC networks, electrical losses are included in the ED model as additional active power loads connected to its two extreme nodes, where each loads represents half of those losses, as shown below:

$$Pac_{i,k}^{loss} = \sum_{m \in i} (0.5) Pac_{im,k}^{loss}; \quad i = 1, \ldots, n_{ac}; k = 1, \ldots, n_{dz} \tag{39}$$

$$Pdc_{j,k}^{loss} = \sum_{n \in j} (0.5) Pdc_{jn,k}^{loss}; \quad j = 1, \ldots, n_{dc}; k, \ldots, n_{dz} \tag{40}$$

E. LINEAR GENERATION COST MODEL

In the ED formulation, the piecewise linear (PWL) technique approximates the quadratic cost generation function by linear segments, as shown in the general equations (41) and (42), while (43) represents the generation limits [20].

$$PG_{g,k} = \sum_{lg=1}^{Lg} \Delta PG_{lg,g,k}; \quad g = 1, \ldots, ng; k = 1, \ldots, n_{dz} \tag{41}$$

$$0 \le \Delta PG_{lg,g,k} \le \left(PG_g^{Max} \Big/ Lg \right); \quad lg = 1, \ldots Lg; g = 1, \ldots, ng; k = 1, \ldots, n_{dz} \tag{42}$$

$$PG_g^{Min} \le PG_{g,k} \le PG_g^{Max}; \quad g = 1, \ldots, ng; k = 1, \ldots, n_{dz} \tag{43}$$

where $PG_{g,k}$ is the active power in generator g located at the dispatch zone k.

F. TRANSMISSION AC/DC NETWORK(S) MODEL

For the sake of simplicity, a linear power flow model for transmission networks is included, involving the matrix [**PTDF**], vectors [**SV**] and [**ENS**], and a vector containing all fictitious nodal power loads, which represent the transmission network electrical losses, denoted as [**Ploss**]. Furthermore, the vector [**Pline**] integrates the transmission element power flows, calculated by equations (44) and (45), and expresses the transmission element limits:

$$[\mathbf{Pline}] = [\mathbf{PTDF}] \{[\mathbf{SV}] + [\mathbf{ENS}] - [\mathbf{Ploss}]\} \tag{44}$$

$$-\left[\mathbf{Pline^{Max}}\right] \le [\mathbf{Pline}] + [\mathbf{Ploss}] \le \left[\mathbf{Pline^{Max}}\right] \tag{45}$$

Furthermore, electrical losses are quadratic functions in terms of the power flow, as indicated in (34); thus, we approximate them to linear functions using a PWL technique. In this study, we propose the same PWL technique used to linearize the generation production costs for electrical loss function linearization. Therefore, for AC transmission networks, the PWL technique application gives equations (46)–(52) for the linear approximation of electrical losses, while similar

equations are (53)−(59) for DC transmission networks [24], [26].

$$Pac_{im,k} = Pac^{+}_{im,k} - Pac^{-}_{im,k}; \quad m \in i; k = 1, \ldots, n_{dz} \tag{46}$$

$$\sum_{l=1}^{L} \Delta Pac_{im,l,k} = Pac^{+}_{im,k} + Pac^{-}_{im,k}; \quad m \in i; k = 1, \ldots, n_{dz} \tag{47}$$

$$0 \le \Delta Pac_{im,l,k} \le \left(Pac^{Max}_{im} \Big/ L\right); \quad m \in i; l = 1, \ldots, L; k = 1, \ldots, n_{dz} \tag{48}$$

$$Pac^{+}_{im,k}, Pac^{-}_{im,k} \ge 0; \quad m \in i; k = 1, \ldots, n_{dz} \tag{49}$$

$$\Delta Pac_{im,l,k} \ge \Delta Pac_{im,l+1,k}; \quad m \in i; l = 1, \ldots, L; k = 1, \ldots, n_{dz} \tag{50}$$

$$Pac^{loss}_{im,k} = r_{im} \sum_{l=1}^{L} sac_{im,l} \Delta Pac_{im,l,k}; \quad m \in i; k = 1, \ldots, n_{dz} \tag{51}$$

where:

$$sac_{im,l} = (2l - 1)\left(Pac^{Max}_{im} \Big/ L\right); \quad m \in i; l = 1, \ldots, L \tag{52}$$

$Pac^{+}_{im,k}$ and $Pac^{-}_{im,k}$ are dummy positive variables representing the power flow in the transmission element from node i to m in the dispatch zone k, and $\Delta Pac_{im,l,k}$, and $sac_{im,l}$ are the corresponding power flow linear segment l, and slope, respectively. Equations (53)−(59) have similar meanings for the linearized electrical losses in the DC networks.

$$Pdc_{jn,k} = Pdc^{+}_{jn,k} - Pdc^{-}_{jn,k}; \quad n \in j; k = 1, \ldots, n_{dz} \tag{53}$$

$$\sum_{l=1}^{L} \Delta Pdc_{jn,l,k} = Pdc^{+}_{jn,k} + Pdc^{-}_{jn,k}; \quad n \in j; k = 1, \ldots, n_{dz} \tag{54}$$

$$0 \le \Delta Pdc_{jn,l,k} \le \left(Pdc^{Max}_{jn} \Big/ L\right); \quad n \in j, ; l = 1, \ldots, L; k = 1, \ldots, n_{dz} \tag{55}$$

$$Pdc^{+}_{jn,k}, Pdc^{-}_{jn,k} \ge 0; \quad n \in j; k = 1, \ldots, n_{dz} \tag{56}$$

$$\Delta Pdc_{jn,l,k} \ge \Delta Pdc_{jn,l+1,k}; \quad n \in j; l = 1, \ldots, L; k = 1, \ldots, n_{dz} \tag{57}$$

$$Pdc^{loss}_{ij,k} = r_{jn} \sum_{l=1}^{L} sdc_{jn,l} \Delta Pdc_{jn,l,k}; \quad n \in j; k = 1, \ldots, n_{dz} \tag{58}$$

where the slope of the linear segment l is:

$$sdc_{jn,l} = (2l - 1)\left(Pdc^{Max}_{jn} \Big/ L\right); \quad n \in j; l = 1, \ldots, L \tag{59}$$

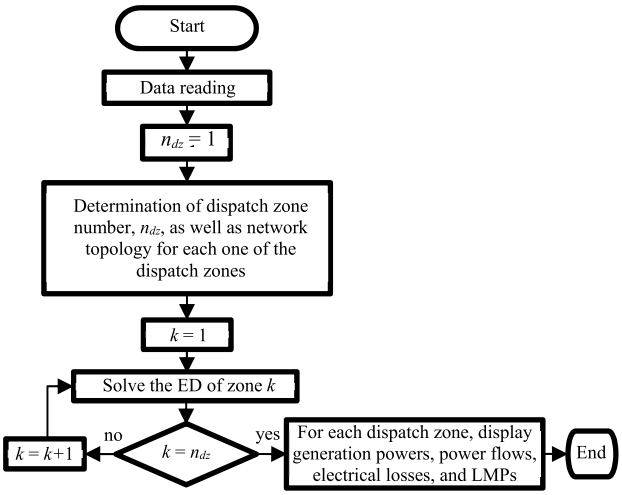

FIGURE 2. General procedure for performing zone allocation and their respective economic dispatch.

Finally, equations (60)−(62) represent the proposal for linearization of the VSC converter electrical losses, formulation based in [24].

$$Pvsc_{v,k} = \sum_{l=1}^{L} \Delta Pvsc_{l,v,k} = B_{VSC}(\theta_i - \phi_v) + (0.5)P^{loss}_{im,k}; \quad v = 1, \ldots, n_{vsc}; k = 1, \ldots, n_{dz} \tag{60}$$

$$0 \le Pvsc^{loss}_{v,k} \le \left(Pvsc^{Max}_{v} \Big/ L\right); \quad v = 1, \ldots, n_{vsc}; k = 1, \ldots, n_{dz} \tag{61}$$

$$Pvsc^{loss}_{v,k} = \alpha_v + \sum_{l=1}^{L} svsc_{l,v} \Delta Pvsc_{l,v,k}; \quad v = 1, \ldots, n_{vsc}; k = 1, \ldots, n_{dz} \tag{62}$$

where the slope of the correspondent linear segment l is given as follows:

$$svsc_{l,v} = (2l - 1)\,\gamma_v \left(Pvsc^{Max}_{v} \Big/ L\right) + \beta_v; \quad v = 1, \ldots, n_{vsc}; l = 1, \ldots, L \tag{63}$$

$Pvsc^{Max}_{v}$ is the maximum power flow through VSC v, and $\Delta Pvsc_{l,v,k}$ is segment l of the VSC v power flow, which pertains to dispatch zone k.

Fig. 2 illustrates the steps involved in the proposed methodology. The first stage refers to the dispatch zone search procedure. Once this procedure is completed, an economical dispatch is executed for each determined dispatch zone. The dispatch zone search algorithm was programmed in Fortran, and the optimization model was solved using GAMS.

Once ED is performed, an analysis of FTR supported bilateral contracts is carried out, with the purpose of showing that these contracts work even when transmission and VSC losses are present with power flow control definition in some VSCs.

Bilateral contracts (BCs) are considered as difference contracts characterized by the specification of a trade price in ($/MWh) between power buyers and sellers and the actual

TABLE 1. PTDFs of the AC/DC-IPS of fig.3.

	AC1				DC		AC2			
	1	2	3	7(VSC1)	9	10	8(VSC2)	6	5	4
1	6.6667	-6.6667	0	0	0	0	0	0	0	0
2	-6.6667	20	-13.3333	0	0	0	0	0	0	0
3	0	-13.3333	26.6667	-13.3333	0	0	0	0	0	0
7(VSC1)	0	0	-13.3333	13.3333	46.8384	-46.8384	0	0	0	0
9	0	0	0	0	1	0	0	0	0	0
10	0	0	0	0	-46.8384	46.8384	0	0	0	0
8(VSC2)	0	0	0	0	0	0	13.3333	-13.3333	0	0
6	0	0	0	0	0	0	-13.3333	26.6667	-13.3333	0
5	0	0	0	0	0	0	0	-13.3333	20	-6.6667
4	0	0	0	0	0	0	0	0	-6.6667	6.6667

TABLE 2. Validation test: power generation (MW), losses (MW), Locational Marginal Prices ($/MWh), total cost ($/h), and error (%).

Variables	SQP	4 segments		8 segments		12 segments		20 segments	
		Results	Error	Results	Error	Results	Error	Results	Error
Pg1	51.47	51.8591	0.7560	51.5273	0.1113	51.5193	0.0958	51.4790	0.0175
Pg2	257.38	257.6365	0.0997	257.3992	0.0075	257.4057	0.0100	257.3868	0.0026
Power Losses	8.8490	9.4956	7.3070	8.9265	0.8758	8.9249	0.8577	8.8658	0.1899
LMP1	8.5147	8.3750	1.6407	8.5625	0.5614	8.6250	1.2954	8.5250	0.1210
LMP2	8.5987	8.4592	1.6223	8.6919	1.0839	8.7117	1.3142	8.6107	0.1396
LMP3	8.5573	8.4347	1.4327	8.6542	1.1324	8.6697	1.3135	8.5658	0.0993
LMP4	8.8295	8.8500	0.2322	8.7750	0.6172	8.8500	0.2322	8.8500	0.2322
LMP5	9.3501	9.3038	0.4952	9.2713	0.8428	9.3038	0.4952	9.3038	0.4952
LMP6	9.4049	9.4162	0.1202	9.3645	0.4296	9.3911	0.1467	9.3861	0.1999
LMP7	8.4849	8.4014	0.9841	8.6031	1.3931	8.6128	1.5074	8.5052	0.2392
LMP8	9.4878	9.5613	0.7747	9.4846	0.0337	9.5035	0.1655	9.4920	0.0443
LMP9	8.4849	8.4014	0.9841	8.6031	1.3931	8.6128	1.5074	8.5052	0.2392
LMP10	8.4125	8.3456	0.7952	8.5174	1.2470	8.5175	1.2481	8.4261	0.1617
Total Cost	2953.1250	2967.4032	0.4835	2955.6934	0.0870	2954.1436	0.0345	2953.5317	0.0138
Average error			1.2663		0.7011		0.7303		0.1568

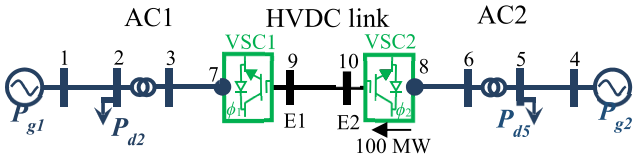

FIGURE 3. AC/DC grid with a two-terminal VSC-HVDC link.

PML of each of the injection/extraction nodes. Assumptions to keep present are (i) FTRs are acquired by consumers, because they suffer more intensively the LMP volatility caused by the load, congestion, and losses impact; (ii) there is a reference LMP put in the BCs; (iii) even though the existence of BCs, producers, and consumers are obligated to participate in the day-ahead market; and (iv) the ISO does not know the negotiated price in all the BCs; thus, they are not able to assign a specific price to the injections/extractions of each contract.

Mathematically, for each BC this can be written as [26]:

$$R_{FTR} = P_{neg}(\pi_{neg} - \pi_G) \tag{64}$$

where R_{FTR} is the payment of the FTR owner located at node D, to the generator at node G, P_{neg} is the negotiated power, and π_{neg}, π_G are the reference LMP and the LMP at node G, respectively. Note that (65) may have a positive, negative, or zero value, depending on the operative condition. Additionally, the payment of the ISO, R_{ISO}, to each FTR owner is defined by the following equation:

$$R_{ISO} = P_{neg}(\pi_D - \pi_G) \tag{65}$$

where π_D is the LMP corresponding to node D.

As will be observed in the studio cases, FTRs are a great alternative for avoiding LMP volatility.

IV. CASES OF STUDY

A. VALIDATION TEST – PROPOSED APPROACH VS SEQUENTIAL QUADRATIC PROGRAMMING

This section comprises a comparative analysis aimed at demonstrating the effectiveness of the proposed optimization method.

The proposed method was applied to a two-terminal VSC-HVDC network interconnecting two independent AC networks, as shown in Fig. 3, the parameters of wich are found in [16]. For validation, the results were compared with those of the Sequential Quadratic Programming (SQP) method reported in the same reference. Additionally, a comparison was conducted using the proposed PWL technique for the nonlinear loss function of the VSCs, distinguishing between the rectifier and inverter. In both cases, linearization tests were performed using four, eight, twelve and twenty line

segments of the nonlinear functions. The matrix BGVSC of this proof system, which was calculated using the methodology described above, is shown in Table 1. Additionally, VSC1 employs the control mode VSC_{Ectrl}, which aims to a maintain constant voltage at node 9, E1, at 2 p.u. On the other hand, VSC2 is under the control mode VSC_{Pctrl}, to inject a controlled power quantity of 100 MW into the HVDC link through node 10.

The nonlinear function data describing the losses of VSCs operating as rectifiers and inverters are $P^{loss}_{vsc\_rec} = 5.25e^{-3} + 1.65e^{-3}\left|P_{vsc,i}\right| + 2.10e^{-3}P^2_{vsc,i}$ p.u. and $P^{loss}_{vsc\_inv} = 5.25e^{-3} + 1.65e^{-3}\left|P_{vsc,i}\right| + 3.14e^{-3}P^2_{vsc,i}$ p.u., respectively [28].

Table 1 depicts the BGVSC matrix containing the network reactances and conductances, as well as the control exerted by VSC1 over the voltage of node 9. Note that this matrix is composed of two diagonal blocks, resulting from the dispatch zone search algorithm. Furthermore, it should be noted that there are 25 different nonzero locations and 75 zero locations. Therefore, in future work, sparsity techniques can be employed to efficiently store each matrix block. After assigning the reference nodes to each dispatch zone, the inverse of the BGVSC matrix must be calculated, and Equations (31) and (32) are used to compute the PTDFs.

An advantage of applying the zone dispatch algorithm is that, in this case, the BGVSC matrix can be divided into two smaller matrices, enabling the handling of large-scale problems and achieving a more efficient computational solution.

The flow control performed by VSC2 is simulated such way that a power extraction equal to the controlled flow plus converter losses is introduced at node 8. Meanwhile, at node 10 of the DC network, a power injection equal to the controlled power flow is introduced.

Table 2 presents the validation of the proposed model, considering the same suppositions as in [16] and without considering the loss curve for the inverter and rectifier. It was observed that a very small error was achieved with 20 segments. In terms of the generation power and total cost, it can be noted that four segments are sufficient; because the respective errors are below 1% and the average error is less than 1.5%. However, more segments should be used when analyzing Locational Marginal Prices (LMP). Therefore, the use of eight segments is proposed, with the goal of LMP errors remaining below 1.5%, and the average error is reduced by approximately half compared to the four segments solution.

Table 3 incorporates the loss curve for the inverter and rectifier, resulting in an increase in the total losses compared to Table 2. When comparing the results of 20 segments with those of four and eight segments in Table 3, the same conclusions as in Table 2 are reached, confirming that a good approximation is achieved with eight segments.

B. DECENTRALIZATION INTO THE CENTRALIZED ECONOMIC DISPATCH

Two test cases were presented using the 3-VSC system previously analyzed in [20], but with some modifications.

TABLE 3. Dispatch test including the loss curve for inverter and rectifier: power generation (MW), losses (MW), LMPs ($/MWH), total cost ($/H), and error (%).

Variables	20 segments	4 segments		8 segments	
	Value	Error	Error	Error	Error
Pg1	52.1186	52.499	0.7299	52.1707	0.1000
Pg2	257.7227	257.9726	0.0970	257.7368	0.0055
Power Losses	9.8413	10.4725	6.4138	9.9075	0.6727
LMP1	8.5250	8.3750	1.7595	8.5625	0.4399
LMP2	8.6107	8.4592	1.7594	8.6919	0.9430
LMP3	8.5720	8.4380	1.5632	8.6594	1.0196
LMP7	8.4957	8.3784	1.3807	8.5883	1.0900
LMP9	8.4957	8.3784	1.3807	8.5883	1.0900
LMP10	8.4168	8.3227	1.1180	8.5028	1.0218
LMP8	9.4278	9.4604	0.3458	9.4070	0.2206
LMP6	9.3552	9.3739	0.1999	9.3294	0.2758
LMP5	9.3038	9.3038	0.0000	9.2713	0.3493
LMP4	8.8500	8.8500	0.0000	8.7750	0.8475
Total Cost	2961.9567	2975.7445	0.4655	2964.1645	0.0745
Average error			1.2295		0.5821

Specifically, the system was duplicated to have two identical systems interconnected through a back-to-back link (BtB), consisting of two VSCs located at node 5. Fig. 4 shows the configuration of the system.

In the first case, it was decided not to use the VSC_{Pctrl} control mode, and the VSC_{Ectrl} control mode was implemented in converters VSC1, VSC6, and VSC7, while the remaining converters were in the $VSC_{\phi ctrl}$ control mode. In the second case, the aim is to demonstrate the use of the dispatch zone assignment algorithm; therefore, the VSC_{Pctrl} control mode has been incorporated in converters VSC2, VSC5, and VSC8. Additionally, the VSC_{Ectrl} mode has been used in converters VSC1, VSC4, and VSC7 and the $VSC_{\phi ctrl}$ mode in converters VSC3 and VSC6. It is important to mention that eight-line segments have been used in the linearized formulation in each test case.

1) CASE 1

In this case, because the VSC_{Pctrl} control mode was omitted, there was only one dispatch zone, that is, the entire system was electrically interconnected, and the ED was solved in a centralized fashion, considering eight linear segments for the PWL technique application. The results are presented in Tables 5 and 6, respectively.

Table 5 shows that all generation units participate in economic dispatch, resulting in higher dispatch allocations to Pg1, Pg4, Pg16, and Pg19 because of their lower generation costs compared to the other units. Some of these units were dispatched to their maximum generation limits. It is important to highlight that in this case, there is no restriction associated with the VSC_{Pctrl} mode; therefore, it is expected that the operational cost will be the most economical.

Because there is only one dispatch zone, in Table 6 it is clear that there exists a certain LMP homogeneity, and the highest difference is between the LMPs of nodes 8 and 16 (9.1268-8.2799 = 0.9069 $/MWh), which is caused by electrical losses, in the absence of congested lines.

TABLE 4. Data of the AC/DC system in Figure 4.

Generator	Pgmax (MW)	Pgmin (MW)	A ($/h)	B ($/MWh)	C ($/MW^{2}h)	Load nodes	P_d (MW)
1, 16	250	0	60	6.4	0.004	3, 6, 18, 21	150
2, 17	100	0	78	8	0.005	7, 8, 9, 22, 23, 24	60
4, 19	250	0	310	7.8	0.002		
5, 20	100	0	78	8	0.005		

AC transmission element parameters (pu)	DC transmission element parameters (pu)
$z_{12} = z_{45} = z_{78} = z_{1617} = z_{1920} = z_{2223} = 0.01 + j0.15$	
$z_{13} = z_{46} = z_{79} = z_{1618} = z_{1921} = z_{2224} = 0.01 + j0.20$	$r_{1314} = r_{2829} = 0.0209$
$z_{23} = z_{56} = z_{89} = z_{1718} = z_{2021} = z_{2231} = z_{2324} = 0.01 + j0.15$	$r_{1315} = r_{2830} = 0.0278$
$z_{310} = z_{533} = z_{611} = z_{912} = z_{1825} = z_{2126} = z_{2427} = z_{3132} = 0.01 + j0.15$	$r_{1415} = r_{2930} = 0.0417$

VSC1 – VSC8 data

Rating		Converter loss curve coefficients (pu)			
S (MVA)	±Vdc (kV)	α	β	γ_{rec}	γ_{inv}
200	100	0.00525	0.00165	0.0021	0.00314

TABLE 5. Dispatch of Case 1: power generation (MW), losses (MW), and total cost ($/H).

Case 1	Pg1	Pg2	Pg4	Pg5	Pg16	Pg17	Pg19	Pg20	**Total Losses**	**Total Power**	**Total Cost**
	250.00	50.00	179.18	62.50	218.75	37.50	150.37	37.50	**25.80**	**985.80**	**8720.14**

TABLE 6. LMP ($/MWH) Case 1.

Node	LMP	Node	LMP	Node	LMP	Node	LMP	Node	LMP	Node	LMP	Node	LMP
1	8.3677	6	8.7024	11	8.7448	16	8.2199	21	8.5528	26	8.5761	31	8.6856
2	8.4704	7	9.1011	12	8.8791	17	8.3207	22	8.7839	27	8.6374	32	8.6336
3	8.6441	8	9.1268	13	8.7238	18	8.4914	23	8.8251	28	8.5512	33	8.6336
4	8.4575	9	9.0106	14	8.7448	19	8.3625	24	8.7401	29	8.5761	34	8.6336
5	8.5916	10	8.7238	15	8.8791	20	8.4177	25	8.5512	30	8.6374		

TABLE 7. BC data for Case 1.

BC	(1) N_{gen}	(2) N_{load}	(3) π_G	(4) π_D	(5) π_{neg}	(6) P_{neg}
1	4	7	8.4575	9.1011	9	60
2	4	8	8.4575	9.1268	9	40
3	19	22	8.3625	8.7839	7	60
4	19	23	8.3625	8.8251	7	40
5	19	18	8.3625	8.4914	9	20

Table 7 displays the data for the five BCs, where N_{gen}, N_{load}, π_G y π_D represent the nodes and LMPs of the participating generators and loads in the BCs, respectively. Meanwhile, π_{neg} and P_{neg} denote the prices and negotiated powers for each BC, respectively.

In columns A - G of Table 8, the operations related to each BC are performed out as follows:

A. The consumer pays the ISO.
B. The ISO pays the generator.
C. The consumer pays the generator for contract-for-differences.
D. ISO collects charges for its FTR.
E. Total payment from the load.
F. Total payment to the generator.
G. ISO payment.

For example, for BC 1, it can be noted that in columns E and F, the calculated amount is equivalent to BC, that is, 9(60) = 540.00. It is also observed that the ISO income in column A corresponds to the payment in column G, resulting in a balance of zero for the ISO.

2) CASE 2

The parameters related to the control modes of VSCs are as follows: In the VSC_{Ectrl} converters, voltages at nodes 13, 28, and 34 are set to 2 pu; in the $VSC_{\phi ctrl}$ converters, the angles at nodes 12 and 27 are set to 0; in the VSC_{Pctrl} converters, the power flows $P_{ctrl}2 = P_{ctrl}5 = 100$ MW and $P_{ctrl}7 = -80$ MW are controlled in converters VSC2, VSC5, and VSC6, respectively.

When using these types of converters, an algorithm to determine the dispatch zones must be applied. In this case, four zones were obtained, as represented in the graph in Fig. 5. A virtual unit called ENS should be added at each dispatch zone to compensate for the generation gap between generators reaching their limits and insufficient to supply

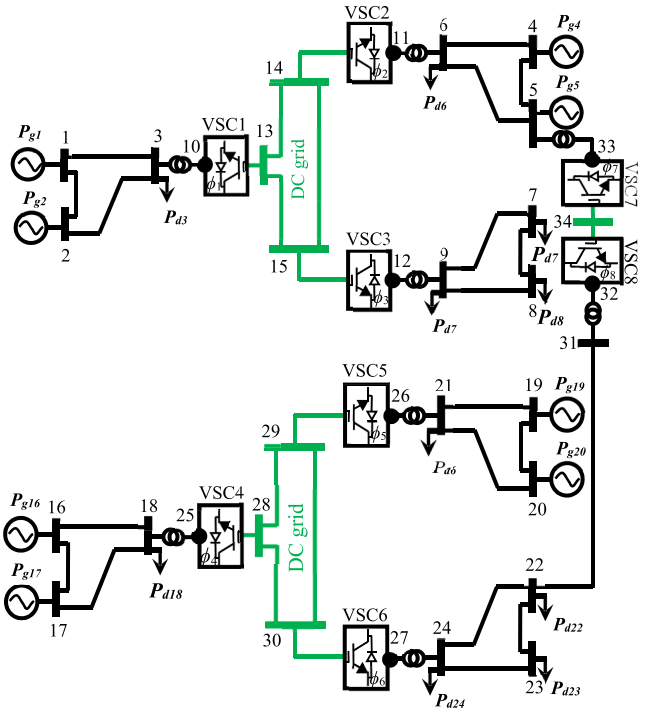

FIGURE 4. AC/DC System for the zone-wise dispatch and global dispatch.

TABLE 8. BC compensation for Case 1.

BC	A	B	C	D	E	F	G
	(4)(6)	(3)(6)	(6) [(5)-(3)]	(6) [(4)-(3)]	A+C-D	B+C	B+D
1	546.07	507.45	32.55	38.6160	540.00	540.00	546.07
2	365.07	338.30	21.70	26.7720	360.00	360.00	365.07
3	527.03	501.75	-81.75	25.2840	420.00	420.00	527.03
4	353.00	334.50	-54.50	18.5040	280.00	280.00	353.00
5	169.83	167.25	12.75	2.5780	180.00	180.00	169.82

TABLE 9. ENS generator data.

Gen	PGmax (MW)	PGmin (MW)	a_g ($/h)	b_g ($/MWh)	c_g ($/MW^{2}h)
ENS	1000	0	0	1000	0

the corresponding load. Table 9 presents data for the virtual units.

Fig. 5 shows the dispatch zone configuration, which allows independent dispatching. It is crucial to note that at each VSC$_{Pctrl}$ terminal, the controlled power flow must be managed as an injection. The AC transmission lines are represented in black; DC transmission lines are depicted in green, and VSC connections are shown in blue.

Once the dispatch zones have been defined, ED is carried out in each of them. Table 10 presents the results of the calculations.

From the active power production results in Table 10, it can be observed that the generation units of each dispatch zone are

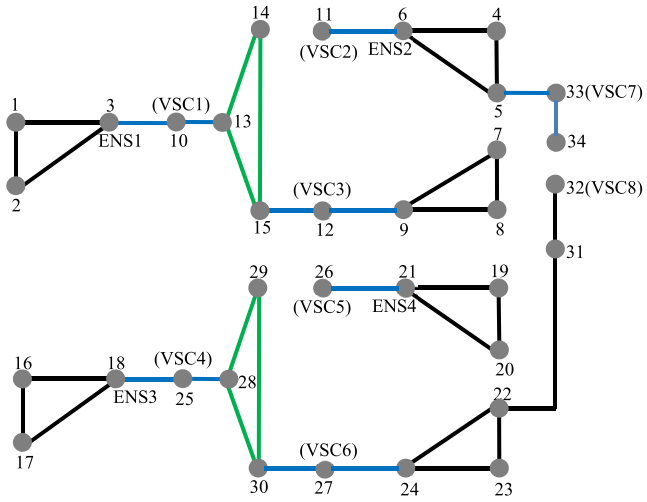

FIGURE 5. Graph for Case 2.

responsible for meeting the demand, losses, and, in the case of being an exporting zone, power injections to other zones.

The injection costs at nodes 14, 29, and 32 are accounted for at their respective LMPs, which leads to an increase of 26.58% in the total cost because network separation prevents centralized dispatch and reduces competition among the existing units in each zone.

Additionally, it is noteworthy that Zone 2 exhibits the highest active power production because it must supply power to Zones 1 and 3. In contrast, Zone 3 shows the lowest active power production as it receives power from Zones 2 and 4.

It is worth noting that, overall, because all generation units were able to fully meet the load and electrical losses at the AC/DC-IPS, there was no need to activate any ENS unit.

Table 11 lists the LMPs for each dispatch zone. The highest values correspond to Zone 2, an exporting zone, because this zone supplies power to Zones 1 and 3. In contrast, Zone 3, an importing zone, exhibits the lowest LMP, because it receives power from Zones 2 and 4, and Zone 3 only needs to dispatch its most economical generation unit (Pg5) to fully meet the demand and cover the losses in its own zone.

In the last part of this case, Table 12 contains the necessary data to calculate the performance of bilateral contracts, as shown in Table 13. It should be noted that even though a generator and a load are involved in a BC, and they pertain to different dispatch zones, the BC continues to function correctly, which is the situation of the generator in node 4 that subscribed BC 1 and BC 2 with consumer at node 7 and consumer at node 8, respectively. The same condition is present between the generator at node 19 and consumers at nodes 18, 22, and 23.

In Table 13, it can be observed that the same payment is reached in columns E and F. Additionally, unlike Table 11, in some elements of column D in Table 13, there are negative values because the load has to pay the ISO for its FTR, indicating that generators charge more than the load's payment. Nevertheless, all the BCs meet the expectations of the generators and consumers involved.

TABLE 10. Dispatch of Case 2: power generation (MW), losses (MW), and total cost ($/H).

	Zone 1		Zone 2		Zone 3		Zone 4		Total losses	Total dispatch	Total cost
Case 2	Pg1	Pg2	Pg4	Pg5	Pg16	Pg17	Pg19	Pg20			
	208.33	30.55	250.00	86.20	156.01	0	187.83	66.67	**25.59**	**985.59**	**11,037.72**

TABLE 11. LMP ($/MWH) of Case 2.

Zone 1				Zone 2		Zone 3				Zone 4	
Node	LMP	Node	LMP	Node	LMP	Node	LMP	Node	LMP	Node	LMP
1	8.1169	7	8.8172	4	8.7728	16	7.5667	24	7.9178	19	8.5500
2	8.2500	8	8.8504	5	8.9167	17	7.6714	23	7.974	20	8.6037
3	8.3920	9	8.7004	6	9.0702	18	7.7712	22	7.9442	21	8.8399
10	8.4421			11	9.1505	25	7.7952	31	7.8259	26	8.9181
13	8.4421			33	8.9698	28	7.7952	32	7.7677		
14	8.4059			34	8.9698	29	7.7701				
15	8.5693					30	7.8285				
12	8.5693					27	7.8285				

TABLE 12. BC data for Case 2.

BC	(1)	(2)	(3)	(4)	(5)	(6)
	N_{gen}	N_{load}	π_G	π_D	π_{neg}	P_{neg}
1	4	7	8.7728	8.8172	9	60
2	4	8	8.7728	8.8504	9	40
3	19	22	8.5500	7.9442	7	60
4	19	23	8.5500	7.9740	7	40
5	19	18	8.5500	7.7712	9	20

TABLE 13. BC compensation for Case 2.

BC	A	B	C	D	E	F	G
	(4)(6)	(3)(6)	(6) [(5)-(3)]	(6) [(4)-(3)]	A+C-D	B+C	B+D
1	529.03	526.37	13.63	2.66	540.00	540.00	529.03
2	354.02	350.91	9.09	3.10	360.00	360.00	354.02
3	476.65	513.00	-93.00	-36.35	420.00	420.00	476.65
4	318.96	342.00	-62.00	-23.04	280.00	280.00	318.96
5	155.42	171.00	9.00	-15.58	180.00	180.00	155.42

V. CONCLUSION

This study makes several significant contributions to the field of economic dispatch in AC/DC-IPS systems, because it proposes the following: (i) a search approach to define dispatch areas, (ii) the inclusion of virtual generators to maintain power balance, (iii) a generalized model for calculating PTDFs, and (iv) the use of the same PWL technique to represent cost and loss curves. These contributions improve automation and demonstrate the efficiency of economic dispatch in AC/DC-IPS systems.

The use of dispatch zones helps manage the economic dispatch problem more efficiently in AC/DC-IPS systems with power flow control converters, by dividing a large-scale problem into smaller ones, thereby reducing the required time and computational effort.

Two case studies were presented, covering both centralized and decentralized economic dispatches, and it was shown that the model adapts correctly to both scenarios.

We can assert that the economic dispatch in the Case 2 is approached in a similar manner to the problem that arises when transmission elements are congested. This can also lead to separation and, consequently, the creation of dispatch zones.

The method of accounting for costs involves adding the results of evaluating the costs of bilateral contracts for energy exchange between generators from one dispatch zone and loads from another dispatch zone.

Regarding the choice of the number of segments to represent the cost and loss curves, it was found that four segments are sufficient to obtain acceptable results from the perspective of generation powers and total cost. However, when seeking a good approximation of LMP, it is recommended to use at least eight segments.

Finally, Financial Transmission Rights (FTRs) in electricity markets are essential for achieving efficient, competitive, and sustainable electricity supply. In this sense, through the two study cases, the applicability of this concept in AC/DC-IPS is helpful to support bilateral contracts, even in cases where there is more than one dispatch zone, and their participants pertain to different dispatch zones.

ACKNOWLEDGMENT

The authors would like to thank the Consejo Nacional de Humanidades Ciencias y Tecnologías (CONAHCYT) for their financial support, which was essential for the completion of this project.

REFERENCES

[1] M. Kahl, C. Freye, and T. Leibfried, "A cooperative multi-area optimization with renewable generation and storage devices," *IEEE Trans. Power Syst.*, vol. 30, no. 5, pp. 2386–2395, Sep. 2015, doi: 10.1109/TPWRS.2014.2363762.

[2] A. Kargarian, Y. Fu, and Z. Li, "Distributed security-constrained unit commitment for large-scale power systems," *IEEE Trans. Power Syst.*, vol. 30, no. 4, pp. 1925–1936, Jul. 2015, doi: 10.1109/TPWRS.2014.2360063.

[3] Z. Li, W. Wu, B. Zhang, and B. Wang, "Decentralized multi-area dynamic economic dispatch using modified generalized benders decomposition," *IEEE Trans. Power Syst.*, vol. 31, no. 1, pp. 526–538, Jan. 2016, doi: 10.1109/TPWRS.2015.2399474.

[4] Z. Li, W. Wu, M. Shahidehpour, and B. Zhang, "Adaptive robust tie-line scheduling considering wind power uncertainty for interconnected power systems," *IEEE Trans. Power Syst.*, vol. 31, no. 4, pp. 2701–2713, Jul. 2016, doi: 10.1109/TPWRS.2015.2466546.

[5] M. Zhou, M. Wang, J. Li, and G. Li, "Multi-area generation-reserve joint dispatch approach considering wind power cross-regional accommodation," *CSEE J. Power Energy Syst.*, vol. 3, no. 1, pp. 74–83, Mar. 2017, doi: 10.17775/CSEEJPES.2017.0010.
[6] M. Khanabadi, Y. Fu, and C. Liu, "Decentralized transmission line switching for congestion management of interconnected power systems," *IEEE Trans. Power Syst.*, vol. 33, no. 6, pp. 5902–5912, Nov. 2018, doi: 10.1109/TPWRS.2018.2838046.
[7] Y. Jia, Z. Y. Dong, C. Sun, and K. Meng, "Cooperation-based distributed economic MPC for economic load dispatch and load frequency control of interconnected power systems," *IEEE Trans. Power Syst.*, vol. 34, no. 5, pp. 3964–3966, Sep. 2019, doi: 10.1109/TPWRS.2019.2917632.
[8] F. J. Nogales, F. J. Prieto, and A. J. Conejo, "A decomposition methodology applied to the multi-area optimal power flow problem," *Ann. Oper. Res.*, vol. 120, nos. 1–4, pp. 99–116, 2003, doi: 10.1023/A:1023374312364.
[9] R. Baldick and D. Chatterjee, "Coordinated dispatch of regional transmission organizations: Theory and example," *Comput. Oper. Res.*, vol. 41, pp. 319–332, Jan. 2014, doi: 10.1016/j.cor.2012.12.016.
[10] H. Narimani, S.-E. Razavi, A. Azizivahed, E. Naderi, M. Fathi, M. H. Ataei, and M. R. Narimani, "A multi-objective framework for multi-area economic emission dispatch," *Energy*, vol. 154, pp. 126–142, Jul. 2018, doi: 10.1016/j.energy.2018.04.080.
[11] C. Barrows, B. McBennett, J. Novacheck, D. Sigler, J. Lau, and A. Bloom, "Multi-operator production cost modeling," *IEEE Trans. Power Syst.*, vol. 34, no. 6, pp. 4429–4437, Nov. 2019, doi: 10.1109/TPWRS.2019.2918849.
[12] X. Li, W. Wang, H. Wang, J. Wu, and Q. Xu, "Flexibility robust optimal operation strategy for cross-regional interconnected power under load-source coordination," *IEEE Access*, vol. 8, pp. 161124–161137, 2020, doi: 10.1109/ACCESS.2020.3020646.
[13] G. Du, D. Zhao, X. Liu, Z. Wu, and C. Li, "Decentralized robust dispatch for multi-area AC/DC system considering wind power uncertainty," *IET Gener., Transmiss. Distrib.*, vol. 15, no. 19, pp. 2710–2721, Oct. 2021, doi: 10.1049/gtd2.12209.
[14] C. Wu, X.-P. Zhang, and M. J. H. Sterling, "Global electricity interconnection with 100% renewable energy generation," *IEEE Access*, vol. 9, pp. 113169–113186, 2021, doi: 10.1109/ACCESS.2021.3104167.
[15] A. B. Kunya, A. S. Abubakar, and S. S. Yusuf, "Review of economic dispatch in multi-area power system: State-of-the-art and future prospective," *Electr. Power Syst. Res.*, vol. 217, Apr. 2023, Art. no. 109089, doi: 10.1016/j.epsr.2022.109089.
[16] L. M. Castro, J. H. Tovar-Hernández, N. González-Cabrera, and J. R. Rodríguez-Rodríguez, "Real-power economic dispatch of AC/DC power transmission systems comprising multiple VSC-HVDC equipment," *Int. J. Electr. Power Energy Syst.*, vol. 107, pp. 140–148, May 2019, doi: 10.1016/j.ijepes.2018.11.018.
[17] L. M. Castro, N. González-Cabrera, D. Guillen, J. H. Tovar-Hernández, and G. Gutiérrez-Alcaraz, "Efficient method for the optimal economic operation problem in point-to-point VSC-HVDC connected AC grids based on Lagrange multipliers," *Electr. Power Syst. Res.*, vol. 187, Oct. 2020, Art. no. 106493, doi: 10.1016/j.epsr.2020.106493.
[18] J. Renedo, A. A. Ibrahim, B. Kazemtabrizi, A. García-Cerrada, L. Rouco, Q. Zhao, and J. García-González, "A simplified algorithm to solve optimal power flows in hybrid VSC-based AC/DC systems," *Int. J. Electr. Power Energy Syst.*, vol. 110, pp. 781–794, Sep. 2019, doi: 10.1016/j.ijepes.2019.03.044.
[19] L. M. Castro, E. Acha, and J. R. Rodriguez-Rodriguez, "Efficient method for the real-time contingency analysis of meshed HVDC power grids fed by VSC stations," *IET Gener., Transmiss. Distrib.*, vol. 12, no. 13, pp. 3158–3166, Jul. 2018.
[20] N. González-Cabrera, L. M. Castro, G. Gutiérrez-Alcaraz, and J. H. Tovar-Hernandez, "Alternative approach for efficient OPF calculations in hybrid AC/DC power grids with VSC-HVDC systems based on shift factors," *Int. J. Electr. Power Energy Syst.*, vol. 124, Jan. 2021, Art. no. 106395, doi: 10.1016/j.ijepes.2020.106395.
[21] J. S. Guzmán-Feria, L. M. Castro, J. H. Tovar-Hernández, N. González-Cabrera, and G. Gutiérrez-Alcaraz, "Unit commitment for multi-terminal VSC-connected AC systems including BESS facilities with energy time-shifting strategy," *Int. J. Electr. Power Energy Syst.*, vol. 134, Jan. 2022, Art. no. 107367, doi: 10.1016/j.ijepes.2021.107367.
[22] J. Dong, Y. Li, Y. Lu, and S. Han, "Accuracy study of linearization methods for quadratic cost curves of thermal units in unit commitment problems," *IET Gener., Transmiss. Distrib.*, vol. 16, no. 11, pp. 2198–2207, Jun. 2022.
[23] J. S. Guzmán-Feria, L. M. Castro, N. González-Cabrera, and J. H. Tovar-Hernández, "Security constrained OPF for AC/DC systems with power rescheduling by power plants and VSC stations," *Sustain. Energy, Grids Netw.*, vol. 27, Sep. 2021, Art. no. 100517, doi: 10.1016/j.segan.2021.100517.
[24] H. Zhang, V. Vittal, G. T. Heydt, and J. Quintero, "A mixed-integer linear programming approach for multi-stage security-constrained transmission expansion planning," *IEEE Trans. Power Syst.*, vol. 27, no. 2, pp. 1125–1133, May 2012, doi: 10.1109/TPWRS.2011.2178000.
[25] N. Alguacil, A. L. Motto, and A. J. Conejo, "Transmission expansion planning: A mixed-integer LP approach," *IEEE Trans. Power Syst.*, vol. 18, no. 3, pp. 1070–1077, Aug. 2003, doi: 10.1109/TPWRS.2003.814891.
[26] D. Z. Fitiwi, L. Olmos, M. Rivier, F. de Cuadra, and I. J. Pérez-Arriaga, "Finding a representative network losses model for large-scale transmission expansion planning with renewable energy sources," *Energy*, vol. 101, pp. 343–358, Apr. 2016, doi: 10.1016/j.energy.2016.02.015.
[27] F. P. Sioshansi, *Competitive Electricity Markets: Design, Implementation, Performance*. Amsterdam, The Netherlands: Elsevier, 2011.
[28] D. S. Kirschen and G. Strbac, *Fundamentals of Power System Economics*, 2nd ed. Washington, DC, USA: Wiley, 2018.
[29] *Cómo surgió la interconexión eléctrica entre Guatemala y México*. Instituto Nacional de Electrificación, disponible en. Accessed: Feb. 11, 2023. [Online]. Available: https://www.inde.gob.gt/como-surgio-la-interconexion-electrica-entre-guatemala-y-mexico/
[30] Q. Zhao, "Technical and economic impact of the deployment of a VSC-MTDC supergrid with large-scale penetration of offshore wind," Ph.D. thesis, Programa de Doctorado en Energía Eléctrica, Universidad Pontificia Comillas, España, 2019. [Online]. Available: https://repositorio.comillas.edu/xmlui/handle/11531/35419?show=full
[31] E. Acha and B. Kazemtabrizi, "A new STATCOM model for power flows using the Newton–Raphson method," *IEEE Trans. Power Syst.*, vol. 28, no. 3, pp. 2455–2465, Aug. 2013, doi: 10.1109/TPWRS.2012.2237186.
[32] A. J. Wood, B. F. Wollenberg, and G. B. Sheblé, *Power Generation, Operation, and Control*, 3rd ed. Hoboken, NJ, USA: Wiley, 2014.
[33] R. J. Wilson, *Introduction To Graph Theory*, 4th ed. London, U.K.: Robin Wilson, 1996.
[34] J. Beerten, S. Cole, and R. Belmans, "A sequential AC/DC power flow algorithm for networks containing multi-terminal VSC HVDC systems," in *Proc. IEEE PES Gen. Meeting*, Minneapolis, MN, USA, Jul. 2010, pp. 1–7, doi: 10.1109/PES.2010.5589968.

OMAR PÉREZ ANDRADE (Member, IEEE) was born in Indaparapeo, Michoacán, Mexico, in 1990. He received the B.S. and M.S. degrees in electrical engineering from the Instituto Tecnológico de Morelia, Michoacán, in 2012 and 2018, respectively, where he is currently pursuing the Ph.D. degree in electrical engineering. His research interests include power systems and electricity markets.

JOSÉ HORACIO TOVAR HERNÁNDEZ (Senior Member, IEEE) was born in Manza, Huaniqueo de Morales, Michoacán, Mexico, in 1958. He received the B.Eng. degree from the Instituto Tecnológico de Morelia, Michoacán, in 1984, and the M.S. and Ph.D. degrees from the Instituto Politécnico Nacional, Mexico, in 1985 and 1995, respectively.

As a professional, he has been a Consultant and the Project Manager in diverse electrical companies and institutions from Mexico and Central America. Since 1993, he has been an Associate Professor with the Instituto Tecnológico de Morelia. His research interests include power systems and electricity markets.

CECILE ALEJANDRA TOVAR RAMÍREZ (Member, IEEE) was born in Morelia, Michoacán, Mexico, in 1984. She received the B.S. and M.S. degrees in electrical engineering from the Instituto Tecnológico de Morelia, Michoacán, in 2009 and 2011, respectively, and the Ph.D. degree in electrical engineering from Universidad Michoacana de San Nicolás de Hidalgo, Morelia, in 2019.

Since 2017, she has been an Associate Professor with the Instituto Tecnológico de Morelia. Her research interests include the analysis of energy systems, the development of coupling models of electricity and primary energy networks, with an emphasis on natural gas networks, and the analysis of energy markets in order to observe the economic impact that their behavior has on electricity prices.